Check for updates

Received: 16 July 2024 | Accepted: 4 September 2024

DOI: 10.1111/imm.13863

ORIGINAL ARTICLE

immunology
Insights into immunity in health and disease

Multiomic-based immune response profiling in migraine, vestibular migraine and Meniere's disease

Pablo Cruz-Granados[1] | **Lidia Frejo**[1,2,3] | **Patricia Perez-Carpena**[2,3,4] | **Juan Carlos Amor-Dorado**[5] | **Emilio Dominguez-Duran**[6] | **Maria Jose Fernandez-Nava**[7,8] | **Angel Batuecas-Caletrio**[7,8] | **Elisheba Haro-Hernandez**[2,3,9] | **Marta Martinez-Martinez**[2,3] | **Jose A. Lopez-Escamez**[1,2,3]

[1]Meniere Disease Neuroscience Research Program, Faculty of Medicine and Health, School of Medical Sciences, The Kolling Institute, University of Sydney, Sydney, New South Wales, Australia

[2]Division of Otolaryngology, Department of Surgery, Instituto de Investigación Biosanitaria, ibs.GRANADA, Universidad de Granada, Granada, Spain

[3]Sensorineural Pathology Programme, Centro de Investigación Biomédica en Red en Enfermedades Raras, CIBERER, Madrid, Spain

[4]Department of Otolaryngology, Hospital Universitario San Cecilio, Instituto de Investigación Biosanitaria, ibs.GRANADA, Granada, Spain

[5]Department of Otolaryngology, Hospital Can Misses Ibiza, Ibiza, Spain

[6]Department of Otolaryngology, Hospital Infanta Luisa, Sevilla, Spain

[7]Department of Otolaryngology, Hospital Universitario Salamanca, Instituto de Investigación Biomédica de Salamanca (IBSAL), Salamanca, Spain

[8]Division of Otolaryngology, Department of Surgery, Universidad de Salamanca, Salamanca, Spain

[9]Department of Otorhinolaryngology, Hospital de Baza, Granada, Spain

Correspondence
Jose A. Lopez-Escamez, Meniere Disease Neuroscience Research Program, Faculty of Medicine and Health, School of Medical Sciences, The Kolling Institute, University of Sydney, 10 Westbourne St, St Leonards, Sydney, NSW 2064, Australia,
Email: jose.lopezescamez@sydney.edu.au

Funding information
Meniere's Society UK, Grant/Award Number: CLINMON-2; University of Sydney, Grant/Award Number:

Abstract

Migraine (MI) is the most common neurological disease, affecting with 20% of the world population. A subset of 25% of MI patients showcase concurrent vestibular symptoms, which may classify as vestibular migraine (VM). Meniere's disease (MD) is a complex inner ear disorder defined by episodes of vertigo associated with tinnitus and sensorineural hearing loss with a significant autoimmune/autoinflammatory contribution, which symptoms overlap with VM. Blood samples from 18 patients with MI (5), VM (5) and MD (8) and 6 controls were collected and compared in a case–control study. Droplet-isolated nuclei from mononuclear cells used to generate scRNAseq and scATACseq data sets from MI,

Abbreviations: ATAC, assay for transposase accessible chromatin; DA, differential accessibility; DC, dendritic cells; DEG, differential expressed genes; DGE, differential gene expression; EC, healthy controls from 10× Genomics Repository; ES, enrichment score; G-CSF, granulocyte colony-stimulating factor; GM-CSF, granulocyte-macrophage colony-stimulating factor; GSEA, gene set enrichment analysis; HC, healthy controls; HGF, hepatocyte growth factor; ILC-1, Type 1 innate immune cells; IREA, immune response enrichment analysis; MD, Meniere's disease; MDMc, Meniere's disease monocyte-driven cluster; MI, migraine; MI + VMc, migraine + vestibular migraine cluster; PBMCs, peripheral blood mononuclear cells; QC, quality control; SCF, stem cell factor; UMAP, Uniform Manifold Approximation and Projection; VEGF, vascular endothelial growth factor; VM, vestibular migraine.

This is an open access article under the terms of the Creative Commons Attribution-NonCommercial-NoDerivs License, which permits use and distribution in any medium, provided the original work is properly cited, the use is non-commercial and no modifications or adaptations are made.
© 2024 The Author(s). *Immunology* published by John Wiley & Sons Ltd.

K7013-B3414G; Instituto de Salud Carlos III, Grant/Award Number: PI20-1126; ISCIII Sara Borrell Postdoctoral Fellowship, Grant/Award Number: CD20/0153

VM and MD. MI and VM have no differences in their immune transcriptome; therefore, they were considered as a single cluster for further analyses. Natural Killer (NK) cells transcriptomic data support a polarisation triggered by Type 1 innate immune cells via the release of interleukin (IL)-12, IL-15 and IL-18. According to the monocyte scRNAseq data, there were two MD clusters, one inactive and one driven by monocytes. The unique pathways of the MI + VM cluster were cellular responses to metal ions, whereas MD monocyte-driven cluster pathways showed responses to biotic stimuli. MI and MD have different immune responses. These findings support that MI and VM have a Type 1 immune lymphoid cell response, and that there are two clusters of MD patients, one inactive and one Monocyte-driven.

KEYWORDS
autoinflammation, cytokines, Meniere disease, migraine, monocytes

INTRODUCTION

Migraine (MI) is a disabling, complex neurological disorder that affects around 20% of the world population, with a higher incidence in women and significant familial aggregation [1]. Epidemiological evidence has estimated that MI heritability is around 42% worldwide, and it is considered a multifactorial trait resulting from interactions between multiple genetic variants and environmental factors [2].

Around 25% of the individuals with MI also show episodic vestibular symptoms, and this syndrome has been defined as vestibular migraine (VM), according to the diagnostic criteria jointly formulated by the International Headache Society and the Barany Society [3]. In addition, both MI and VM show a familial aggregation [4]. The concurrence of episodic vertigo and MI is also observed in Meniere's disease (MD) [5], a chronic inflammatory disorder of the inner ear defined by episodes of vertigo associated with fluctuating sensorineural hearing loss, tinnitus and aural fullness [6]. All these overlapping conditions are defined according to the symptoms reported by patients; of note, there is a gap in knowledge in the immune response in these disorders, and the immune profile has seldom been investigated, and no molecular markers for MI, VM or MD have been consistently found.

The immune response and cytokine dysregulation play significant roles in VM, MD, MI and their interplay. Studies show that pro-inflammatory cytokines like interleukin (IL)-1β, IL-6, Tumor Necrosis Factor (TNF)-α and IL-8 are elevated in patients with MI, while anti-inflammatory cytokines may be decreased [7, 8]. However, the overall picture from serum or plasma studies during MI attacks has not provided a consistent pattern regarding inflammatory cytokines [9, 10]. Several studies have indicated that MD patients exhibit high basal levels of IL-1β, leading to elevated levels of cytokines and chemokines. Interestingly, transcriptomics and single-cell immune profiling in peripheral blood mononuclear cells (PBMCs) have defined two different endophenotypes in MD based on their cytokine profiles; one linked to cytokines suggesting a Type 2 immune response associated with high levels of IL-4 and IgE [11, 12] and the other with high levels of IL-1β supporting autoinflammation [13].

Flook et al. described that how gene expression in PBMCs showed significant differences in MD and VM patients, and logistic regression identified that IL-1β, CCL3, CCL22 and CXCL1 levels could differentiate them [14]. In addition, differences in the levels of specific cytokines like CCL18, CCL3 and CXCL4 have been noted between patients with MD or MI and controls, suggesting distinct immune responses in MI, VM and MD [15].

The intricate relationship between these conditions underscores the importance of understanding the immune response and cytokine profiles to improve diagnostic accuracy and develop targeted treatment strategies for patients affected by VM, MD or both. Thus, this study aims to define a molecular signature in mononuclear cells in patients with MI, VM and MD by single-cell transcriptomics and to determine if patients with VM have a specific immune profile or share the MI or the MD signature.

METHODOLOGY

Patient cohort and sample collection

The Granada Clinical Research Ethics Review Board approved the protocol for this study (PI17/1644; PI20-1126), and the informed consent was obtained in all participants.

13652567, 0, Downloaded from https://onlinelibrary.wiley.com/doi/10.1111/imm.13863 by Universidad De Granada, Wiley Online Library on [25/09/2024]. See the Terms and Conditions (https://onlinelibrary.wiley.com/terms-and-conditions) on Wiley Online Library for rules of use; OA articles are governed by the applicable Creative Commons License

The clinical features of patients with MI, VM and MD are shown in Supplementary eTable 1. Blood samples were obtained from 24 Spanish participants with no diagnosed allergies or autoimmune diseases (8 patients with MD, 5 with VM, 5 with MI and 6 healthy controls). In addition, four single-cell PBMC-filtered matrix files were retrieved from the 10× Genomics public repository and used as a second set of controls [16–19].

Nuclei isolation from frozen PBMCs

The isolation procedure was optimized from nuclei isolation from PBMCs (CG000365) for Chromium Next GEM Single-Cell Multiome ATAC + Gene Expression (CG000338; 10× Genomics, Pleasanton, CA, USA) [20, 21]. Briefly, PBMCs were thawed and diluted in RPMI + 10% fetal bovine serum, and cells were counted. To eliminate granulocytes with extracellular DNA, we sorted cells stained in CD66 (FACSAria III Cell Sorter, BD, Bioscience, Frankling Lakes, NJ, USA). We continued to isolate the nuclei from a million cells per sample. Briefly, we centrifuged cells (300 rcf for 5 min at 4°C). The supernatant was removed, replaced with 1 mL refrigerated lysis buffer and incubated for 3 min before resuspension. The nuclei were centrifuged again (500 rcf for 5 min at 4°C). The pellet was resuspended in 1 mL diluted nuclei buffer and passed through a 40-μm cell strainer. All steps were performed se on ice. Nuclei were stained and counted. Nuclei were collected into 10% bovine serum albumin. Next, 1 U/mL RNase inhibitor (Sigma-Aldrich, 03335402001) was added to all final solutions.

Multiome library preparation and sequencing

Single-cell multiome libraries for healthy controls and patients with MI, VM and MD were prepared using "Chromium Next GEM Single-Cell Multiome ATAC + Gene Expression" (CG000338; 10× Genomics). Nuclei were transposed in a bulk solution before being into a tube with Gel Beads-in-Emulsion (GEMs) into a tube. Barcoding was performed during reverse transcription on the transposed DNA (ATAC) and the cDNA (RNA). Both RNA and ATAC libraries were generated from amplified cDNA and transposed DNA, respectively.

Pair-end sequencing for the 24 samples was performed by using a Hiseq X Illumina sequencing platform (San Diego, CA, USA). The cellranger-arc mkfastq function from Cell Ranger ARC V.2.0.0 was used to demultiplex Illumina's base calling files (BCL) into a FASTQ format for downstream analysis.

Single-cell RNA sequencing analysis

FASTAQ files were analysed using Cell Ranger ARC v.2.0.2 and aligned with GRCh38 for the human genome reference, as per 10× Genomics guidelines [22], to generate a filtered matrix file for downstream analysis. Samples with lower unique molecular identifiers quantity than recommended by the HTML summary were left out of the downstream analysis [23].

The filtered matrix output files were loaded in R and analysed using the default pipeline of the package *Seurat* v.4.1.4 for downstream analysis and visualization [24, 25]. The pipeline was run twice per sample, first with internal controls and then with the external data set to control batch effects. A filter was applied to all samples only to keep cells with ≥200 features and <10% MT genes [26], and for clustering, Uniform Manifold Approximation and Projection (UMAP) generation was chosen [27], UMAP clusters were manually and automatically annotated, using a combination of Azimuth cell markers and FindAllMarkers function, and *Celldex* (MonacoImmuneData) and *SingleR* packages, respectively [25, 28, 29].

Differential expressed genes (DEGs) were retrieved using the *Seurat* FindMarkers function along with *limma* v3.56.2 between condition and controls, and a filter of ±1.5 log2FC and ≤0.05 adjusted *p*-value was applied.

Determining clusters and reclassification

Hierarchical clustering was performed using R's *hclust* function on the DEG analysis lists per cell type, including six MD, five MI and four VM samples. Four samples were excluded as they did not pass the quality controls. For cluster analysis, the Euclidean method was used with both "average" and "centroid" distances [24].

Gene set enrichment analysis and immune response enrichment analysis

Gene set enrichment analysis (GSEA) was performed using single-cell transcriptomic data and the DEG lists obtained from each cluster. For this, *ClusterProfiler* v.4.8.3 package in R was used along with the genome-wide annotation for Human species "org.Hs.eg.db" v3.17.0 (http://org.hs.eg/) [30]. In addition, we also performed immune response enrichment analysis (IREA) by using the DEG data sets according to the IREA tool from the Immune Dictionary [31].

13652567, 0, Downloaded from https://onlinelibrary.wiley.com/doi/10.1111/imm.13863 by Universidad De Granada, Wiley Online Library on [25/09/2024]. See the Terms and Conditions (https://onlinelibrary.wiley.com/terms-and-conditions) on Wiley Online Library for rules of use; OA articles are governed by the applicable Creative Commons License

Single-cell ATAC sequencing analysis

FASTAQ files were analysed using Cell Ranger ARC v.2.0.2 and aligned with GRCh38 for the human genome reference, as per 10× Genomics guidelines [22], to generate a peak coordinates, peak fragments cell metadata files for downstream analysis.

Seurat v.5.1.0 and Signac v1.12.0 were used for downstream analysis [32, 33]. Quality control was based on library features with the following settings: (a) peaks and fragments files were loaded in R and were analysed using quantitative and qualitative analyses. (b) Both, MI + VMc and MDMc ATAC analyses were done following the "Merging Objects and" and "Visualization of Genomic Regions" pipeline and to identify the cell populations the Reference Mapping and RNA Imputation from "scATAC-seq data integration" pipeline was followed, both from the Signac package v1.12.0 [33].

The integrated pre-processed and cell-labelled MI + VM and MD scRNAseq data sets were used as a reference. The quantitative analysis in differential accessibility (DA) used the FindMarkers function to identify differentially accessible peaks between conditions and controls.

The qualitative analysis was performed using differentially expressed reference genes for each cell type-specific polarisation state caused by cytokines according to IREA. Chromatin accessibility graphs were plotted for each cluster and both sets of controls.

RESULTS

The number of cells found in MI, VM, MD and HC did not differ amongst B cells, CD^{4+}, NK cells and monocytes. The only exeption was CD^{8+} cells that showed a borderline significance after Bonferroni correction (Supplementary eTable 2).

MI and VM cannot be differentiated according to their single-cell immune profile

The cellular distribution of CD^{4+}, CD^{8+}, B cells, NK cells and monocytes did not differ between MI (Figure 1a) and VM (Figure 1b) patients, according to their scRNAseq data obtained. When we compared the number of shared and non-shared DEGs for each cell type, we observed that the monocyte population has the highest number of DEGs compared to the other cell populations, with 99 and 61 being unique to MI (beige) and VM (brown), respectively, and 36 shared between them (Figure 1c);

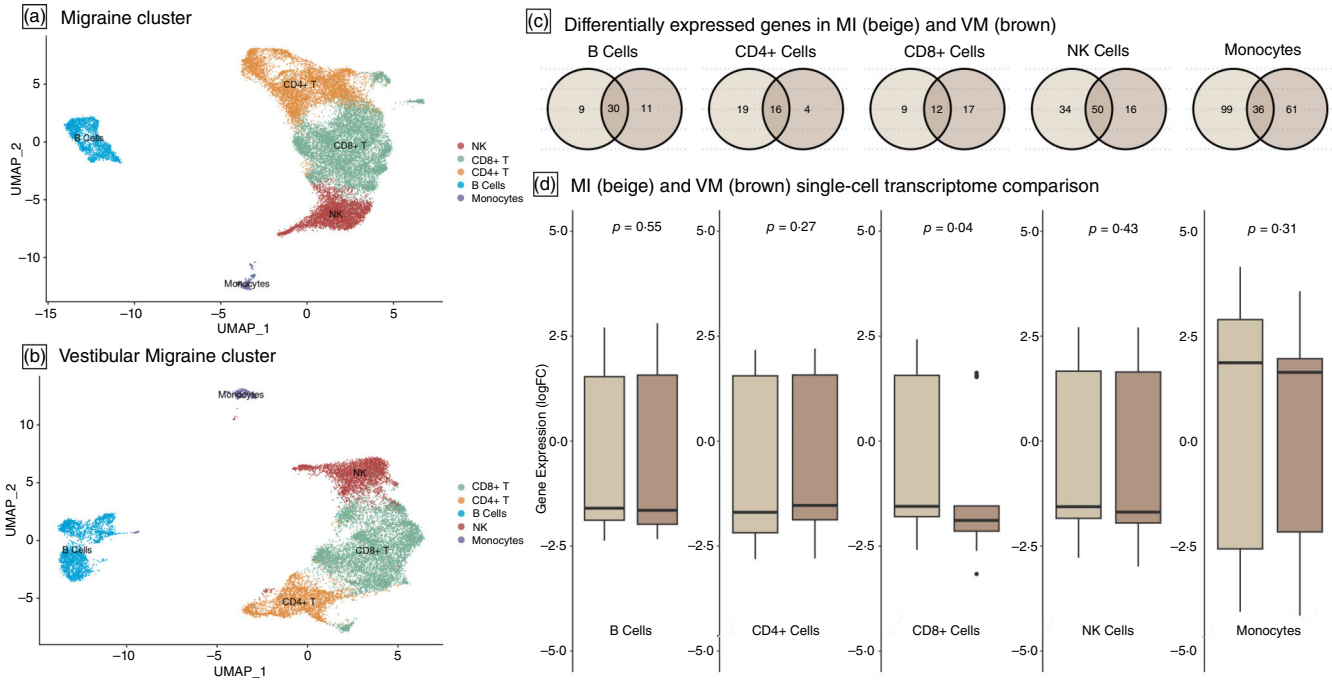

FIGURE 1 (a) Integrated UMAP in the MI cluster with colour coded cell identification of five subpopulations (CD^{4+} T cells, CD^{8+} T cells, B cells, NK cells, monocytes). (b) Integrated UMAP in VM with colour coded cell identification of five subpopulations. (c) Venn diagrams differentially expressed genes between MI (beige) and VM (brown) clusters per cell subpopulation. (d) Boxplots of differentially expressed genes using log2FC between both clusters. CD^{8+} T cells population of cells shows slight significantly differences in the gene expression profile for each cluster. MI, migraine; UMAP, Uniform Manifold Approximation and Projection; VM, vestibular migraine.

13652567, 0, Downloaded from https://onlinelibrary.wiley.com/doi/10.1111/imm.13863 by Universidad De Granada, Wiley Online Library on [25/09/2024]. See the Terms and Conditions (https://onlinelibrary.wiley.com/terms-and-conditions) on Wiley Online Library for rules of use; OA articles are governed by the applicable Creative Commons License

however, differences were observed only in the CD^{8+} population when the transcriptomes of each cell population found in MI and VM were compared (Figure 1d). The dendrogram obtained by using scRNAseq data showed no significant differences between VM and MI PBMCs, and for this reason, we merged their scRNAseq data sets for further analyses (see dendrograms in e-Figure 1 and eFigure 2) We termed MI + VMc the newly merged data set, including MI and VM samples. After performing quality control (QC) and filtering, 17 218 cells remained in the MI cluster (MI + VMc), 11 129 cells in the HC and 8347 cells in the EC group.

The main upregulated DEGs observed between MI + VMc and controls in monocytes were *NKA1N2*, *ABCC4*, *ID2*, *FCGR3A* and *SLC24A3*; conversely, the downregulated genes found were *S100A9*, *S100A8*, *TTC7A, PRAM1*, *IRF1*, *NEAT1* and *FOSB* (Supplementary eTable 3).

Two clusters of MD patients are defined according to their single-cell immune profile

When the immune profiles were hierarchically clustered using the "average" method (Supplementary eFigure 3), a large cluster of five patients and a small cluster of two patients were observed in MD according to scRNAseq data sets. A "centroid" clustering method was used (Supplementary eFigure 4) which confirmed that the patient clustering was correct.

The distribution of CD^{4+}, CD^{8+}, B cells, NK cells and monocytes between both MD clusters did not differ. Only 21 DCs were found in the MD inactive cluster, therefore no DGE analysis could be performed, and they were excluded from further analysis (Figure 2a,b).

The large cluster was termed "Inactive" (grey) as it shows only nine DEG compared to both sets of controls. Meanwhile, the second cluster had a significant number of DEG in monocytes, and we named it "Meniere's disease monocyte-driven cluster" (MDMc, blue; Figure 2c).

After QC and filtering, when we compared MDMc-HC, 1340 cell remained in the MDMc and 8965 cells in HCs. On the other hand, when we compared MDMc-EC, MDMc had 948 cells and EC had 8171 cells.

For MD inactive compared to HC, there were 8166 cells in MD Inactive and 11 308 cells in HC. Meanwhile there were 8353 cells in MD Inactive and 9940 cells in EC.

Statistical difference between the Inactive MD and the MDMc was found in the CD^{4+} cells when the scRNA-seq transcriptome was compared (Figure 2d). There were 135 upregulated and 149 downregulated genes in the

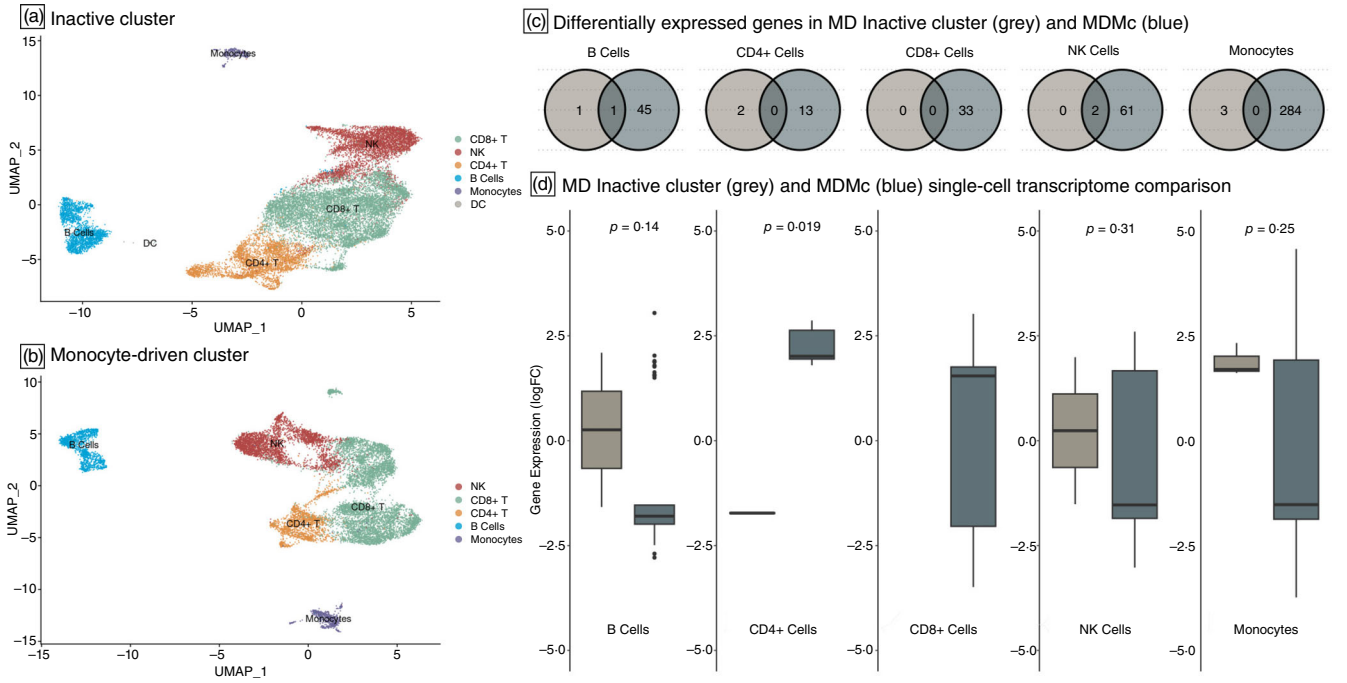

FIGURE 2 (a) Integrated UMAP in the MD monocyte-driven cluster with colour coded cell identification of five subpopulations (CD^{4+} T cells, CD^{8+} T cells, B cells, NK cells, monocytes). (b) Integrated UMAP in the MD inactive cluster with colour coded cell identification of five subpopulations. (c) Venn diagrams showing differentially expressed genes between inactive (grey) and MDMc (blue) clusters per cell subpopulation. (d) Boxplots of differentially expressed genes using log2FC between both clusters. CD^{4+} T cells show a significantly different gene expression profile for each cluster. MD, Meniere's disease; MDMc, Meniere's disease monocyte-driven cluster; UMAP, Uniform Manifold Approximation and Projection.

13652567, 0, Downloaded from https://onlinelibrary.wiley.com/doi/10.1111/imm.13863 by Universidad De Granada, Wiley Online Library on [25/09/2024]. See the Terms and Conditions (https://onlinelibrary.wiley.com/terms-and-conditions) on Wiley Online Library for rules of use; OA articles are governed by the applicable Creative Commons License

MDMc. In this cluster, the main upregulated genes in monocytes were *SDC2*, *RAPGEF1*, *TPRG1*, *ABCC1*, *IL1R1*, *IL1R2*, *IL1RN*, *CXCL8*, *IL3RA* and *CSF2R* conversely; monocytes showed downregulation of *THEM121L*, *FOXP1*, *CD74*, *CD36*, *HLA-DRA*, *IL15* and *CSF3R* (Supplementary eTable 4).

Monocyte-driven MD and MI clusters show differential immune cellular responses

When shared and non-shared genes between MI + VMc and MDMc were compared, we observed the lowest number of mutual genes is found in the CD^{4+} population with no DEGs and the highest number of joint genes in the monocytes with 103 DEGs (Figure 3a).

Box plots comparing the single-cell transcriptomes of each cell population between MI + VM and MD showed that CD^{4+} cells had a distinctive gene expression profile (Figure 3b).

The main DEGs in CD^{4+} cells found in the MI + VMc were *SPON1*, *NELL2*, *TPT1*, *S100A4*, *S100A9* and *BCL2*; conversely, *NPR2*, *KCNK9*, *CDKN1A*, *NDRG2* and *FGD4* were the main DEGs in CD^{4+} cells found in MDMc (Supplementary eTables 5 and 6).

MI and monocyte-driven clusters exhibit different active biochemical pathways

When we compared the shared and non-shared genes of the MDMc and the MI + VMc, there was a higher

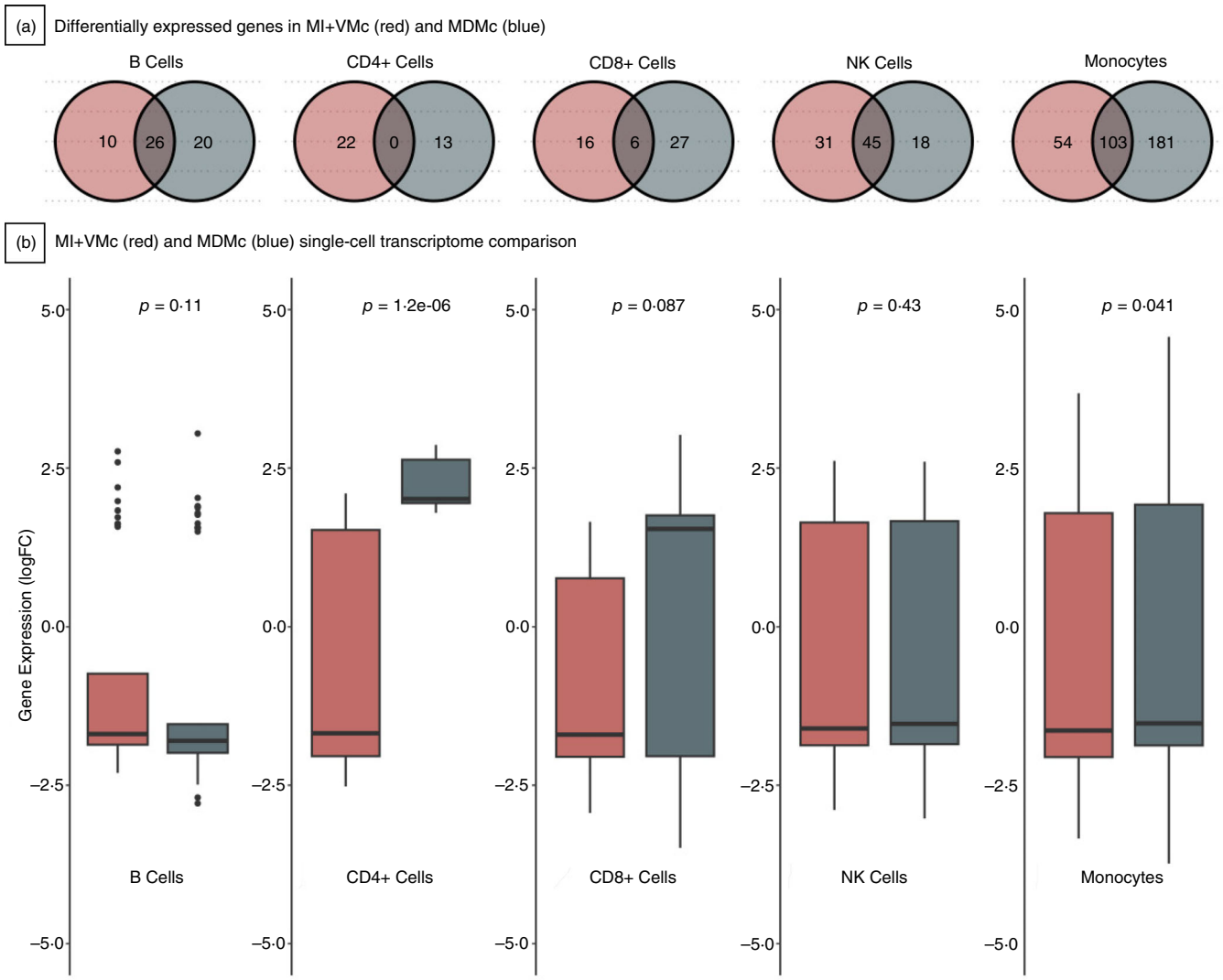

FIGURE 3 (a) Venn diagrams of differentially expressed genes between MI + VMc (red) and MDMc (blue) per cell subpopulation. (b) Boxplots of differentially expressed genes using log2FC MI + VMc and MDMc. CD^{4+} T cells show a significantly differences and monocyte show slight significant differences in the gene expression profile for each cluster. MDMc, Meniere's disease monocyte-driven cluster; MI + VMc, migraine + vestibular migraine cluster.

13652567, 0, Downloaded from https://onlinelibrary.wiley.com/doi/10.1111/imm.13863 by Universidad De Granada, Wiley Online Library on [25/09/2024]. See the Terms and Conditions (https://onlinelibrary.wiley.com/terms-and-conditions) on Wiley Online Library for rules of use; OA articles are governed by the applicable Creative Commons License

(a) Differentially expressed genes between MDMc and MI+VMc

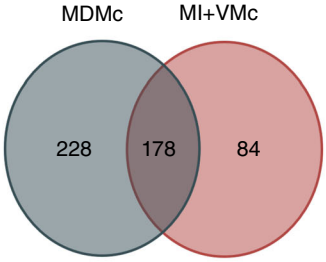

(b)-(c) Possible active biochemical pathwas in MI+VMc and MDMc

Pathways	adjusted p-value
Monocyte-Driven Cluster	
Response to biotic stimulus	7·26E-05
Response to external biotic stimulus	7·71E-05
Response to other organism	7·71E-05
Cytokine production	1·30E-04
Regulation of cytokine production	1·30E-04
MI+VM Cluster	
Cellular response to inorganic substance	1·97E-04
Cellular response to metal ion	1·97E-04
Cellular response to calcium ion	1·97E-04
Glycosyltransferase activity	1·25E-03
Cellular response to salt	2·10E-03

FIGURE 4 (a) Venn diagram total differentially expressed genes between MI + VMc and MDMc. (b) Unique enriched pathways for monocyte-driven cluster by adjusted *p*-value, show a cellular response to inorganic substances such as metal ions. (c) Unique pathways for MI + VM cluster by adjusted *p*-value show a response to external biotic factors. MDMc, Meniere's disease monocyte-driven cluster; MI + VMc, migraine + vestibular migraine cluster.

proportion of non-shared DEG in the MDMc than there was in the MI + VMc cluster (Figure 4a). When the MD inactive cluster was compared with MI + VMc, it showed very few shared differentially expressed genes in all cell types (Supplementary eFigure 5A,B).

The top three enriched pathways according to the GSEA in both the MI + VMc and MDMc were immune system process (GO:0002376), immune response (GO:0006955) and regulation of cellular response to growth factor stimulus (GO:00900287) (Supplementary eTables 7 and 8). When filtered for unique enriched pathways in the MI + VMc, we found that they are driven by a cellular response to inorganic substance (GO:0071241, adjusted *p*-value = $1.97E^{-04}$) and cellular response to metal (GO:0071248, adjusted *p*-value = $1.97E^{-04}$) or Ca^{2+} (GO:0071277, adjusted *p*-value = $1.97E^{-04}$) (Figure 4b); on the other hand, the MDMc unique enriched pathways are driven by a response to a biotic stimulus (GO:0009607, adjusted *p*-value = $7.26E^{-05}$), response to other organisms (GO:0051707, adjusted *p*-value = $7.71E^{-05}$) and cytokine production (GO:0001816, adjusted *p*-value = $1.30E^{-04}$) (Figure 4c).

MI and monocyte-driven clusters have different upstream cytokine pathways

IREA predicted potential cytokines that can trigger polarisation states in both the MI + VMc and MDMc. The NK cell population of the MI + VMc appears to be affected the most, with polarised state NK-e being activated. The cytokines that have the highest enrichment score (ES) are IL-15 (ES = 0.344, adjusted *p*-value = $2.90E^{-05}$), IL-12 (ES = 0.281, adjusted p-value = $4.46E^{-05}$) and IL-2 (ES = 0.250, adjusted *p*-value = $3.27E^{-04}$) (Supplementary eFigure 6 and eTable 9). Conversely, in the MDMc all polarised states appear to be active on the monocytes, with the main growth factors being stem cell factor (SCF) (ES = 0.392, adjusted *p*-value = $3.17E^{-02}$), vascular endothelial growth factor (VEGF) (ES = 0.354, adjusted *p*-value = $3.17E^{-02}$) and hepatocyte growth factor (ES = 0.332, adjusted *p*-value = $5.32E^{-02}$) (Supplementary eFigure 7 and eTable 10).

Single-cell ATAC sequencing confirms gene expression changes in single-cell RNA sequencing data

In Figure 5a,b, it can be observed that the *GZMB* coding sequence (cds) accessibility levels were lower on the NK cells on the MI + VMc compared to the HC in chromosome 14 around 24 634 000 and 24 635 000 base pairs. A similar trend can be observed for other DGEs in the MI + VMc that are biomarkers for the NK-e polarised state (eFigures 8–33).

On the other hand, DA shows that the regions on chromosome 14 between 24 633 830 and 24 634 948 base pairs are downregulated (log2FC = −0.923, adjusted *p*-value = $1.28E^{-12}$), partly validating what is seen in the chromatin accessibility graphs (Supplementary eTable 11). It also shows two other exons that are 4000 and 5000 bp aways from *GZMB* that are slightly upregulated (log2FC = 0.220, adjusted *p*-value = 1.00) and downregulated (log2FC = −0.438, adjusted *p*-value =$7.86E^{-01}$), respectively. Similar results are observed when MI + VMc is compared to EC (Supplementary eTable 12).

We observed that MDMc genes found as biomarkers for polarised states predicted by IREA follow a similar trend as the MI + VMc genes when DA was performed against both set of controls. (Supplementary eTables 13 and 14).

13652567, 0, Downloaded from https://onlinelibrary.wiley.com/doi/10.1111/imm.13863 by Universidad De Granada, Wiley Online Library on [25/09/2024]. See the Terms and Conditions (https://onlinelibrary.wiley.com/terms-and-conditions) on Wiley Online Library for rules of use; OA articles are governed by the applicable Creative Commons License

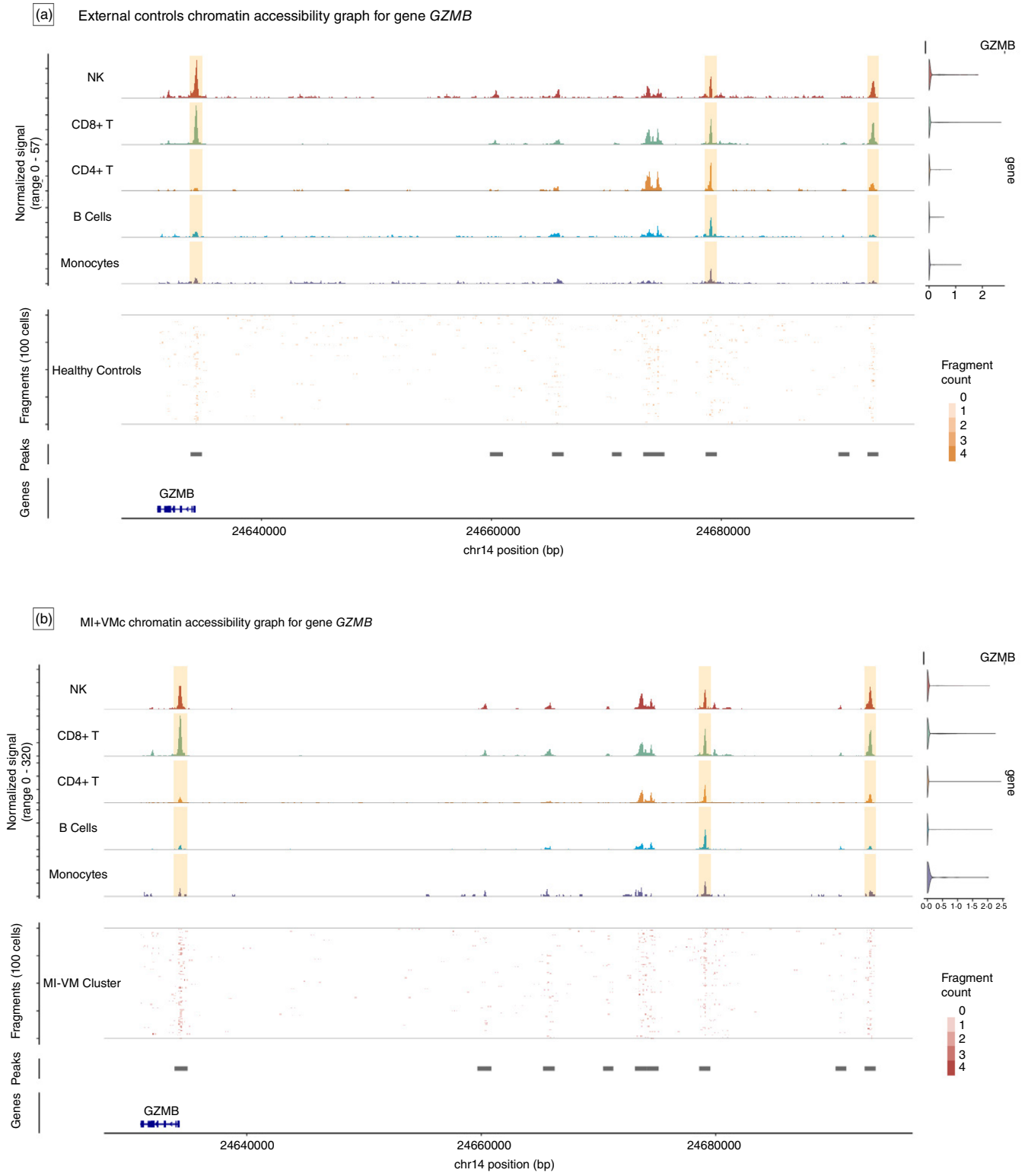

FIGURE 5 (a) Chromatin accessibility of the GZMB gene in healthy controls, separated by cell subpopulation. (b) Chromatin accessibility of *GZMB* in MI + VMc, separated by cell subpopulation. MI + VMc, migraine + vestibular migraine cluster.

DISCUSSION

Our single-cell data in PBMCs support the same immune profile in MI and VM, but also define an immune signature for a subset of MD patients that show a differential gene expression in monocytes, the MDMc.

Although epidemiological research underlines an association between these disorders, transcriptomic data

13652567, 0, Downloaded from https://onlinelibrary.wiley.com/doi/10.1111/imm.13863 by Universidad De Granada, Wiley Online Library on [25/09/2024]. See the Terms and Conditions (https://onlinelibrary.wiley.com/terms-and-conditions) on Wiley Online Library for rules of use; OA articles are governed by the applicable Creative Commons License

and IREA algorithms support divergent etiological triggers [34, 35].

While the precise pathophysiology of both VM and MD remains incompletely elucidated, MI has been linked to MD [36]. Although MD pathophysiology is associated with endolymphatic hydrops, cytokine and other immune mediators in MI or MD emerge as credible triggers for cochlear and vestibular damage in the inner ear leading to vestibular symptoms in both VM and MD. In addition, there is a strong link between neurotological symptoms and MI, with auditory or vestibular dysfunction associated with MI being a common cause of spontaneous episodic vertigo [37]. Therefore, this study aimed to identify specific molecular patterns in PBMCs in individuals with VM, MI and MD using single-cell transcriptomics to improve diagnostic accuracy and find potential therapeutic targets.

MI has an inflammatory response mediated by NK cells. Using IREA, we hypothesise that IL-12, IL-15 and IL-18 can polarise NK cells to NK-e.

A previous study, it was found that these cytokines were produced by dendritic cells and affect NK cells, boosting the immune response. In turn, NK cells produce INF-γ, which primes DCs [38]. In MI patients, our transcriptomic data in NK cells support a polarisation to NK-e that would trigger Type 1 innate immune cells (ILC-1) by releasing IL-12, IL-15 and IL-18. Moreover, IL-2 in conjunction to IL-15, has been found to induce *STAT5*, an important regulator of NK cells development, maturation and cytotoxic function [38].

Furthermore, our results show an upregulation of *CXCL8* (also known as IL-8) in the monocytes of the MI + VMc, which is driven by the feedback of monocyte-released IL-15 [39]. CXCL-8 was found upregulated in the serum of patients that suffer from MIs compared to controls; another study reported higher concentrations of CXCL-8 in blood serum in MI samples collected after 2- to 4-h post-attack onset [9, 40]. Moreover, CXCL-8 was also upregulated in patients who suffer from trigeminal neuralgia, suggesting a potential role in its development [41].

Our data indicate that IL-15 (as IREA predicts) is polarising NK cells and monocytes in patients with MI, and these cells are probably releasing IL-8 in the blood.

Our results also show an upregulation of IL-1β's receptor, *IL1RN*. One study found an upregulation of *IL1RN* after cortical spreading depression in mice, which could be an attempt to regulate the IL-1β inflammatory response [42].

The anti-inflammatory factor *CSF3* (G-CSF) was downregulated in the MI + VMc. In a study in rats, it was found that G-CSF enhances IL-10 through the mTOR/p70S6K pathway, thus reducing inflammatory cytokines IL-1β and TNF-α [43].

Our scATACseq data show that *IL1RN* and *CSF3R* are downregulated compared to controls.

One thing worth mentioning, is that the gene expression of the receptors for the inflammatory growth factor *CSF2* (GM-CSF), *CSF2RA*, *CSF2RB* and *IL3RA* are downregulated when the MI + VMc is compared to EC. GM-CSF and IL-3 are known cytokines involved in activating monocytes, and differentiation into other cell types such as macrophages and dendritic cells [44]. GM-CSF was found to be present in the development of inflammation in autoimmune diseases such as rheumatoid arthritis and multiple sclerosis [45]. IL-3 has not been found to play a role in the aforementioned diseases, but it is present, alongside GM-CSF, in allergic asthma [46].

Taken together, these findings support a systemic ILC-1 response in MI patients, which is mediated by IL-1β, IL-15 and CXCL-8, downregulation of G-CSF, GM-CSF and IL-3, and polarisation of NK cells to NK-e mediated by IL-2, IL-12, IL-15 and IL-18.

Several mechanisms are involved in MD, including IgE-mediated response [11, 12] and autoinflammation [47, 48].

For MD, two subtypes were confirmed by hierarchically clustering MD using an "average" and "centroid" distance methods. The inactive cluster showed few DGEs scattered around all cell types, and most of them are regulatory genes; meanwhile, the number of DGEs in the MDMc were mainly found in the monocytes. A previous study showed that patients had clustered into two subtypes according to the levels of cytokines in PBMCs, where MDL (Meniere's disease low) has a low amount of DGEs compared to controls, MDH (Meniere's disease high) has over 1000 DGEs compared to controls, and the same trend can be observed in differentially methylated CpGs using whole genome bisulphite sequencing [49].

On the monocytes of MDMc, we also observe an upregulation of *IL1RN* and *IL1R2*, which are well-documented [50] decoy receptors for IL-1β, reducing bioavailability and lowering inflammation. These findings confirm previous studies in MD reporting two subtypes according to the immune profile, one being considered autoinflammatory and mediated by overexpression of IL-1β [13].

In the MDMc, we also observed a downregulation of IL-15 and an upregulation of *CXCL8* compared to the controls. IL-15 is known to induce the production of *CXCL8* in monocytes [39]. Previous studies have found that a high *CXCL8*, HGF and G-CSF are linked to the formation of neutrophil extracellular traps that could have a possible role in the pathology of MD [51].

In this study, we did not identify growth factors expressed in PBMC, yet IREA predicts that SCF, VEGF and HGF are present in blood serum and polarising monocytes in the MDMc.

13652567, 0, Downloaded from https://onlinelibrary.wiley.com/doi/10.1111/imm.13863 by Universidad De Granada, Wiley Online Library on [25/09/2024]. See the Terms and Conditions (https://onlinelibrary.wiley.com/terms-and-conditions) on Wiley Online Library for rules of use; OA articles are governed by the applicable Creative Commons License

Both SCF and VEGF also been associated with other inflammatory diseases [52, 53].

VEGF was found to be regulated by TNF-α and IL-6 in patients with rheumatoid arthritis [54], and it was found to be present in significantly higher serum levels in MI patients compared to the controls [53].

In another study, SCF also known as mast cell growth factor was found to be, alongside VEGF, to be regulated by TNF-α, to be produced by keratinocytes, resulting in a worsening of the inflammation in the skin in psoriasis patients [55]. These findings support that patients in MDMc have an autoinflammatory phenotype.

Contrary to MI + VMc, our single-cell data in the MDMc show that *CSF2RA* and *IL3RA* are upregulated. This could indicate that the development of inflammation between MI and MD differs, with GM-CSF and IL-3 being present and monocytes being differentiated into macrophages and DCs.

On the other hand, similar to the MI + VMc, MDMc scRNAseq results show that G-CSF is downregulated, contributing to the inflammation of the disease.

These findings support there is an autoinflammatory phenotype in the MDMc, mediated by IL-1β that associates other growth factors, cytokines and chemokines.

Our GSEA results indicate that MI + VMc has active pathways related to an immune response to inorganic substances and metal ions, whereas the MDMc has active pathways related to biotic factors. These results suggest that MI + VMc and MDMc have different triggers for developing an inflammatory response.

This study has some limitations. First, this experimental procedure is based on isolated nuclei from PBMCs, and granulocytes were not included. Second, the sample size was limited to a few individuals in each group, although the number of cells in each cluster ranges from 948 to 17 318. Finally, the isolated nuclei for scATACseq on each sample were not the same as those isolated for scRNAseq, and combined analyses were not possible at the single-cell level.

CONCLUSION

MI has a Type 1 immune lymphoid cell response, with NK cells polarised to NK-e by cytokines IL-2, IL-12, IL-15 and IL-18. The VM transcriptome does not differ from MI in PBMCs. Conversely, MD consists of two clusters: one mediated by monocytes with an autoinflammatory response with high levels of IL-1β and a second one that is inactive.

ACKNOWLEDGEMENTS

We would like to acknowledge Pablo Martinez-Rodriguez and Jesus Vela for their technical support in sample preparation for single-cell RNA sequencing and single-cell ATAC sequencing. We would also like to acknowledge the patients for donating blood to contribute to this study. Open access publishing facilitated by The University of Sydney, as part of the Wiley - The University of Sydney agreement via the Council of Australian University Librarians.

FUNDING INFORMATION

This research has been funded by K7013-B3414G Grant from University of Sydney, PI20-1126 grant from ISCIII by FEDER Funds from the EU and CLINMON-2 from the Meniere's Society UK. Lidia Frejo was supported by ISCIII Sara Borrell Postdoctoral Fellowship (CD20/0153).

CONFLICT OF INTEREST STATEMENT

The authors declare no conflicts of interest.

DATA AVAILABILITY STATEMENT

The data that support the findings of this study are openly available in Gene Expression Omnibus at https://www.ncbi.nlm.nih.gov/geo/. All data generated in this study are available at Gene Expression Omnibus (GEO) under the accession number are GSE269114 and GSE269117.

ORCID

Pablo Cruz-Granados https://orcid.org/0009-0003-1699-3617
Lidia Frejo https://orcid.org/0000-0002-6104-0941
Patricia Perez-Carpena https://orcid.org/0000-0003-2722-4947
Juan Carlos Amor-Dorado https://orcid.org/0000-0001-9749-8607
Maria Jose Fernandez-Nava https://orcid.org/0000-0002-8997-2687
Angel Batuecas-Caletrio https://orcid.org/0000-0003-2613-670X
Elisheba Haro-Hernandez https://orcid.org/0000-0003-0806-1206
Jose A. Lopez-Escamez https://orcid.org/0000-0002-8583-1430

REFERENCES

1. Bjornsdottir G, Chalmer MA, Stefansdottir L, Skuladottir AT, Einarsson G, Andresdottir M, et al. Rare variants with large effects provide functional insights into the pathology of migraine subtypes, with and without aura. Nat Genet. 2023;55:1843–53.
2. Grangeon L, Lange KS, Waliszewska-Prosół M, Onan D, Marschollek K, Wiels W, et al. Genetics of migraine: where are we now? J Headache Pain. 2023;24:12.
3. Lempert T, Olesen J, Furman J, Waterston J, Seemungal B, Carey J, et al. Vestibular migraine: Diagnostic criteria. J Vestib Res. 2022;32:1–6.

13652567, 0, Downloaded from https://onlinelibrary.wiley.com/doi/10.1111/imm.13863 by Universidad De Granada, Wiley Online Library on [25/09/2024]. See the Terms and Conditions (https://onlinelibrary.wiley.com/terms-and-conditions) on Wiley Online Library for rules of use; OA articles are governed by the applicable Creative Commons License

4. Paz-Tamayo A, Perez-Carpena P, Lopez-Escamez JA. Systematic review of prevalence studies and familial aggregation in vestibular migraine. Front Genet. 2020;11:954.
5. Dlugaiczyk J, Lempert T, Lopez-Escamez JA, Teggi R, von Brevern M, Bisdorff A. Recurrent vestibular symptoms not otherwise specified: clinical characteristics compared with vestibular migraine and Menière's disease. Front Neurol. 2021;12:674092.
6. Lopez-Escamez JA, Carey J, Chung WH, Goebel JA, Magnusson M, Mandalà M, et al. Diagnostic criteria for Menière's disease. J Vestib Res. 2015;25:1–7.
7. Fu C, Chen Y, Xu W, Zhang Y. Exploring the causal relationship between inflammatory cytokines and migraine: a bidirectional, two-sample Mendelian randomization study. Sci Rep. 2023;13:19394.
8. Musubire AK, Cheema S, Ray JC, Hutton EJ, Matharu M. Cytokines in primary headache disorders: a systematic review and meta-analysis. J Headache Pain. 2023;24:36.
9. Duarte H, Teixeira AL, Rocha NP, Domingues RB. Increased interictal serum levels of CXCL8/IL-8 and CCL3/MIP-1α in migraine. Neurol Sci. 2015;36:203–8.
10. Han D. Association of serum levels of calcitonin gene-related peptide and cytokines during migraine attacks. Ann Indian Acad Neurol. 2019;22:277–81.
11. Flook M, Escalera-Balsera A, Rybakowska P, Frejo L, Batuecas-Caletrio A, Amor-Dorado JC, et al. Single-cell immune profiling of Meniere disease patients. Clin Immunol. 2023;252:1–10.
12. Zhang N, Lyu Y, Guo J, Liu J, Song Y, Fan Z, et al. Bidirectional transport of IgE by CD23 in the inner ear of patients with Meniere's disease. J Immunol. 2022;208:827–38.
13. Frejo L, Lopez-Escamez JA. Cytokines and inflammation in Meniere disease. Clin Exp Otorhinolaryngol. 2022;15:49–59.
14. Flook M, Frejo L, Gallego-Martinez A, Martin-Sanz E, Rossi-Izquierdo M, Amor-Dorado JC, et al. Differential proinflammatory signature in vestibular migraine and Meniere disease. Front Immunol. 2019;10:1229.
15. Moleon MDC, Martinez-Gomez E, Flook M, Peralta-Leal A, Gallego JA, Sanchez-Gomez H, et al. Clinical and cytokine profile in patients with early and late onset Meniere disease. J Clin Med. 2021;10:4052.
16. 10× Genomics. PBMC from a healthy donor—No Cell Sorting (10k) Single Cell Multiome ATAC + Gene Expression Dataset by Cell Ranger ARC 1.0.0. 2020 Sep 9.
17. 10× Genomics. PBMC from a healthy donor—No Cell Sorting (3k) Single Cell Multiome ATAC + Gene Expression Dataset by Cell Ranger ARC 1.0.0. 2020 Sep 9.
18. 10× Genomics. PBMC from a healthy donor—No Cell Sorting (10k) Single Cell Multiome ATAC + Gene Expression Dataset by Cell Ranger ARC 2.0.0. 2021 May 3.
19. 10× Genomics. PBMC from a healthy donor—No Cell Sorting (3k) Single Cell Multiome ATAC + Gene Expression Dataset by Cell Ranger ARC 2.0.0, 10× Genomics. 2021 May 3.
20. Sandoval L, Mohammed Ismail W, Mazzone A, Dumbrava M, Fernandez J, Munankarmy A, et al. Characterization and optimization of multiomic single-cell epigenomic profiling. Genes (Basel). 2023;14:1245.
21. Oelen R, de Vries DH, Brugge H, Gordon MG, Vochteloo M, Ye CJ, et al. Single-cell RNA-sequencing of peripheral blood mononuclear cells reveals widespread, context-specific gene expression regulation upon pathogenic exposure. Nat Commun. 2022;13:3267.
22. 10× Genomics. Cell ranger ARC 2.0.2.
23. Luecken MD, Theis FJ. Current best practices in single-cell RNA-seq analysis: a tutorial. Mol Syst Biol. 2019;15:e8746.
24. R Core Team. R: a language and environment for statistical computing. Vienna, Austria: R Foundation for Statistical Computing 4.4.1; 2024 Available from: https://www.R-project.org/
25. Hao Y, Hao S, Andersen-Nissen E, Mauck WM, Zheng S, Butler A, et al. Integrated analysis of multimodal single-cell data. Cell. 2021;184:3573–3587.e29.
26. Osorio D, Cai JJ. Systematic determination of the mitochondrial proportion in human and mice tissues for single-cell RNA-sequencing data quality control. Bioinformatics. 2021;37:963–7.
27. Zhai Z, Lei YL, Wang R, Xie Y. Supervised capacity preserving mapping: a clustering guided visualization method for scRNA-seq data. Bioinformatics. 2022;38:2496–503.
28. Monaco G, Lee B, Xu W, Mustafah S, Hwang YY, Carré C, et al. RNA-Seq signatures normalized by mRNA abundance allow absolute deconvolution of human immune cell types. Cell Rep. 2019;26:1627–1640.e7.
29. Aran D, Looney AP, Liu L, Wu E, Fong V, Hsu A, et al. Reference-based analysis of lung single-cell sequencing reveals a transitional profibrotic macrophage. Nat Immunol. 2019;20:163–72.
30. Wu T, Hu E, Xu S, Chen M, Guo P, Dai Z, et al. Yu, clusterProfiler 4.0: a universal enrichment tool for interpreting omics data. Innovation. 2021;2:100141.
31. Cui A, Huang T, Li S, Ma A, Pérez JL, Sander C, et al. Dictionary of immune responses to cytokines at single-cell resolution. Nature. 2023;625:377–84. https://doi.org/10.1038/s41586-023-06816-9
32. Hao Y, Stuart T, Kowalski MH, Choudhary S, Hoffman P, Hartman A, et al. Dictionary learning for integrative, multimodal and scalable single-cell analysis. Nat Biotechnol. 2023;42:293–304. https://doi.org/10.1038/s41587-023-01767-y
33. Stuart T, Srivastava A, Madad S, Lareau CA, Satija R. Single-cell chromatin state analysis with Signac. Nat Methods. 2021;18:1333–41.
34. Kim SY, Lee CH, Yoo DM, Kwon MJ, Kim JH, Kim JH, et al. Association between Meniere disease and migraine. JAMA Otolaryngol Head Neck Surg. 2022;148:457–64.
35. Chen JY, Guo ZQ, Wang J, Liu D, Tian E, Guo JQ, et al. Vestibular migraine or Meniere's disease: a diagnostic dilemma. J Neurol. 2023;270:1955–68.
36. Pyykkö I, Manchaiah V, Färkkilä M, Kentala E, Zou J. Association between Ménière's disease and vestibular migraine. Auris Nasus Larynx. 2019;46:724–33.
37. Cal R, Bahmad F. Migraine associated with auditory-vestibular dysfunction summary. Braz J Otorhinolaryngol. 2008;74:606–18.
38. Gotthardt D, Sexl V. STATs in NK-cells: the good, the bad, and the ugly. Front Immunol. 2017;7:694.
39. Badolato R, Ponzi AN, Millesimo M, Notarangelo LD, Musso T. Interleukin-15 (IL-15) induces IL-8 and monocyte chemotactic protein 1 production in human monocytes. Blood. 1997;90:2804–9.

13652567, 0, Downloaded from https://onlinelibrary.wiley.com/doi/10.1111/imm.13863 by Universidad De Granada, Wiley Online Library on [25/09/2024]. See the Terms and Conditions (https://onlinelibrary.wiley.com/terms-and-conditions) on Wiley Online Library for rules of use; OA articles are governed by the applicable Creative Commons License

40. Sarchielli P, Alberti A, Vaianella L, Pierguidi L, Floridi A, Mazzotta G, et al. Chemokine levels in the jugular venous blood of migraine without aura patients during attacks. Headache. 2004;44:961–8.
41. Evangelin J, Sherwood IA, Abbott PV, Uthandakalaipandian R, Velu V. Influence of different irrigants on substance P and IL-8 expression for single visit root canal treatment in acute irreversible pulpitis. Aust Endod J. 2020;46:17–25.
42. Lombardo SD, Mazzon E, Basile MS, Cavalli E, Bramanti P, Nania R, et al. Upregulation of IL-1 receptor antagonist in a mouse model of migraine. Brain Sci. 2019;9:172.
43. Dumbuya JS, Chen L, Shu SY, Ma L, Luo W, Li F, et al. G-CSF attenuates neuroinflammation and neuronal apoptosis via the mTOR/p70SK6 signaling pathway in neonatal hypoxia-ischemia rat model. Brain Res. 2020;1739:146817.
44. Ushach I, Zlotnik A. Biological role of granulocyte macrophage colony-stimulating factor (GM-CSF) and macrophage colony-stimulating factor (M-CSF) on cells of the myeloid lineage. J Leukoc Biol. 2016;100:481–9.
45. Cook AD, Louis C, Robinson MJ, Saleh R, Sleeman MA, Hamilton JA. Granulocyte macrophage colony-stimulating factor receptor α expression and its targeting in antigen-induced arthritis and inflammation. Arthritis Res Ther. 2016;18:287.
46. Borriello F, Galdiero MR, Varricchi G, Loffredo S, Spadaro G, Marone G. Innate immune modulation by GM-CSF and IL-3 in health and disease. Int J Mol Sci. 2019;20:834.
47. Zhang DG, Yu WQ, Liu JH, Kong LG, Zhang N, Song YD, et al. Serum/glucocorticoid-inducible kinase 1 deficiency induces NLRP3 inflammasome activation and autoinflammation of macrophages in a murine endolymphatic hydrops model. Nat Commun. 2023;14:1249.
48. Frejo L, Gallego-Martinez A, Requena T, Martin-Sanz E, Amor-Dorado JC, Soto-Varela A, et al. Proinflammatory cytokines and response to molds in mononuclear cells of patients with Meniere disease. Sci Rep. 2018;8:5974.
49. Flook M, Escalera-Balsera A, Gallego-Martinez A, Espinosa-Sanchez JM, Aran I, Soto-Varela A, et al. DNA methylation signature in mononuclear cells and proinflammatory cytokines may define molecular subtypes in sporadic Meniere disease. Biomedicine. 2021;9:1530.
50. Zheng Y, Humphry M, Maguire JJ, Bennett MR, Clarke MCH. Intracellular interleukin-1 receptor 2 binding prevents cleavage and activity of interleukin-1α, controlling necrosis-induced sterile inflammation. Immunity. 2013;38:285–95.
51. Zou J, Zhao Z, Song X, Zhang G, Li H, Zhang Q, et al. Elevated G-CSF, IL8, and HGF in patients with definite Meniere's disease may indicate the role of NET formation in triggering autoimmunity and autoinflammation. Sci Rep. 2022;12:16309.
52. Lukacs NW, Kunkel SL, Strieter RM, Evanoff HL, Kunkel RG, Key ML, et al. The role of stem cell factor (c-kit ligand) and inflammatory cytokines in pulmonary mast cell activation. Blood. 1996;87:2262–8.
53. Mozafarihashjin M, Togha M, Ghorbani Z, Farbod A, Rafiee P, Martami F. Assessment of peripheral biomarkers potentially involved in episodic and chronic migraine: a case-control study with a focus on NGF, BDNF, VEGF, and PGE2. J Headache Pain. 2022;23:3.
54. Macías I, Garcí-Pérez S, Ruiz-Tudela M, Medina F, Chozas N, Giron-Gonzales JA. Modification of pro- and antiinflammatory cytokines and vascular-related molecules by tumor necrosis factor-α blockade in patients with rheumatoid arthritis. J Rheumatol. 2005;32:2102–8.
55. Zhou XY, Chen K, Zhang JA. Mast cells as important regulators in the development of psoriasis. Front Immunol. 2022;13:1022986.

SUPPORTING INFORMATION

Additional supporting information can be found online in the Supporting Information section at the end of this article.

How to cite this article: Cruz-Granados P, Frejo L, Perez-Carpena P, Amor-Dorado JC, Dominguez-Duran E, Fernandez-Nava MJ, et al. Multiomic-based immune response profiling in migraine, vestibular migraine and Meniere's disease. Immunology. 2024. https://doi.org/10.1111/imm.13863

13652567, 0, Downloaded from https://onlinelibrary.wiley.com/doi/10.1111/imm.13863 by Universidad De Granada, Wiley Online Library on [25/09/2024]. See the Terms and Conditions (https://onlinelibrary.wiley.com/terms-and-conditions) on Wiley Online Library for rules of use; OA articles are governed by the applicable Creative Commons License